The Effectiveness of Least Mean Squared-Based Adaptive Algorithms for Active Noise Control System in a Small Confined Space

Francesco Mori [1,*] , Andrea Santoni [1], Patrizio Fausti [1], Francesco Pompoli [1], Paolo Bonfiglio [2] and Pietro Nataletti [3]

1   Department of Engineering, University of Ferrara, 44122 Ferrara, Italy
2   Materiacustica s.r.l., 44122 Ferrara, Italy
3   National Institute for Insurance against Accidents at Work (INAIL), Monte Porzio Catone, 00078 Rome, Italy
*   Correspondence: francesco.mori@unife.it

Abstract: Active noise control (ANC) is a technique applied to eliminate an unwanted sound by superposing a signal of equal amplitude and opposite phase, sometimes defined as an anti-noise signal, computed through an adaptive algorithm. The study described herein aims to evaluate and compare the performance of some of the most popular algorithms based on the least mean squares (LMS) approach applied to a multichannel active noise control system in a small, enclosed space. The comparison is conducted through an experimental evaluation of the ANC algorithms' performance, carried out on a tractor cabin in a hemi-anechoic chamber, generating the unwanted sound field using a dodecahedron sound source placed outside the enclosure, emitting narrowband and broadband signals. The experimental analysis and the comparison with the results obtained in a free field condition have made it possible to show certain practical limitations when implementing the algorithms. The results show that the feed-forward systems allow for greater stability, avoiding the acoustic feedback from the control loudspeakers to the reference microphone when this is outside the cabin, while the feedback system is the slowest configuration to converge, requiring an internal modeling of the reference signal. With random signals, the feed-forward systems concentrate their performance in the range above 500 Hz, while the feedback system becomes ineffective.

Keywords: active noise control; multichannel systems; LMS; enclosure

1. Introduction

An active noise control (ANC) system consists of an electroacoustic device designed to eliminate an unwanted sound by superposing a signal of equal amplitude and opposite phase, sometimes defined as an anti-noise signal, computed through an adaptive algorithm. This technology was proposed and patented by Lueg in 1936, but the development of ANC systems started only in the 1980s with the arrival of digital signal processors (DSPs) on the market [1]. In recent decades, ANC has attracted significant interest for applications in several fields [2,3], where traditional solutions are not very effective due to the low-frequency range of the disturbance. Indeed, ANC is typically used to cancel noise at low frequency, where a low sampling rate makes it possible to process the measured data and generate the output signal in real time.

Four main configurations of active noise control systems can be found in the literature, mainly depending on the type of source of unwanted noise and on the a priori knowledge of the kind of noise emitted [4]. In a feed-forward ANC system, a reference sensor (such as a microphone or an accelerometer) measures the signal of the annoying sound source. The implementation of this ANC configuration is convenient and widely applied whenever it is possible to sense a noise signal coherent with the source to be attenuated. Nevertheless, this is not always possible or convenient, and in such cases, a feedback configuration is

preferable. This other approach does not use a reference sensor but models the reference signal from the sensing of the error signal; thus, this type of system works well for a predictable noise signal, as in the case of periodic signals. Hybrid ANC configurations combine the feed-forward approach to control broadband noise with a feedback algorithm dedicated to narrowband components [5,6]. When the noise source signal is known a priori, ANC configurations with filter coefficients fixed in time rather than computed in real time through an adaptive algorithm can also be used [7,8].

The performance of the ANC system strongly depends on the type of application. For example, in an enclosed space, in which the modal response of the cavity creates a complex acoustic field, the ANC systems suffer from the presence of reflections related to the cavity boundaries, generally limiting the attenuation capacity. In this case, multiple control sources and error microphones are necessary to control the noise, optimizing their position to avoid placing them in pressure nodes [4]. However, only a few applications of multichannel ANC systems in enclosures can be found in the literature. In particular, these studies are mainly related to the field of transport. For example, in the automotive industry, where research is imprinted to find light solutions to limit the increment in fuel consumption respecting the volumetric constraints, the target is to cancel the noise perceived inside the car compartment [9]. One of the typical strategies regards the implementation of the Least Mean Squares algorithm with a filtered reference signal (FXLMS) and its variations, which represents the most common choice in practical applications for its simplicity of implementation and robustness. This is usually employed for engine noise attenuation not only on cars [10,11] but also on work vehicles such as tractors [12,13], harvester machines [14] or loader machines [15]. Other types of noise sources, such as road noise, have a broadband nature but have some characteristics independent of the vehicle speed. In this case, also to limit stability problems, the main strategy regards the use of fixed precalculated filter coefficients [7,16]. Some more innovative algorithms can be found in the literature [17], but they are limited to experimental tests in the laboratory. Even if these LMS-based algorithms have been widely developed in recent decades, a fair comparison among different algorithms in a multichannel configuration applied to an enclosed space is still missing in the literature.

This article aims to experimentally evaluate and compare the effectiveness of some of the most popular adaptive algorithms based on the LMS procedure. The experimental comparison, unlike computer simulations, makes it possible to observe the different behaviors and the limits in implementing the algorithms on a real-time target (timing, memory, latency, ...) and the effectiveness of the ANC system with regard to the imperfections in the positioning of the loudspeakers and the error microphones. The analysis and comparison of the performances are carried out for a $1 \times 2 \times 2$ multichannel configuration, where the first digit represents the number of reference sensors (one microphone), the second digit is the number of control sources (two loudspeakers), and the last one is the number of control sensors (two microphones). In particular, three algorithms are developed in feed-forward configuration: the typical filtered-X LMS (FXLMS), which implements finite impulse response (FIR) filters to model the adaptive coefficients; the algorithm FXNLMS, a variation of the standard FXLMS with a normalized step-size [18–22], in which the parameter for the coefficients updating varies with the power of the filtered reference signal; a recursive version of FXLMS, called filtered-U recursive LMS (FURLMS), which implements infinite impulse response (IIR) filters for the adaptive coefficients [23,24]. It should be stated that the application of this last algorithm is still missing for a multichannel configuration in an enclosed space. Moreover, a feedback configuration of FXLMS is studied, in which two reference signals are internally modeled, starting from the error signals [25,26]. The experimental tests were carried out in a small enclosed space in a hemi-anechoic chamber, with the target of attenuating the noise signal of a simulated source at the ears position of a dummy torso. The choice of a tractor cabin as a case study is related to two larger projects (BRIC 2019 ID-14 and BRIC 2022 ID-11), in which this study is inserted. This analysis represents a preliminary step to reach the final target of these projects: the development

of an ANC system for the reduction of noise exposure of tractor drivers. However, the conclusions found in this experimental study in the hemi-anechoic chamber are intended to be of a general nature for a multichannel ANC system in any confined space.

In Section 2, the schematic representation of the LMS-based algorithms and their analytical development are described. Section 3 illustrates the experimental setup adopted for the tests and the main frequency response functions. Finally, the results of the experimental comparison for several kinds of noise signals and the conclusions are reported in the last two sections respectively, assessing the algorithm's performance in terms of speed of convergence, attenuation, and stability.

2. Description of the LMS-Based Algorithms

The LMS algorithm was introduced by Widrow et al. in 1960 [27] and nowadays represents one of the most popular adaptive algorithms for its simplicity of implementation and robustness. It consists of the minimization of a cost function, which is usually defined as the energy measured at error microphones for ANC applications. This operation is mathematically translated in an explicit algorithm based on a single time step method (Euler's forward formula), used to iteratively update the adaptive filter coefficients at each time instant, starting from the previous instant. This method is conditionally stable due to its explicit nature; thus, it is necessary to properly set the step-size parameter in order to achieve numerical stability. Moreover, another type of stability must be considered in relation to the fact that the basic LMS algorithm does not take into consideration the delay introduced by the wave propagation from the control loudspeaker to the error microphone. To take into account this delay, the reference signal is filtered for the impulse response calculated between the control source and the microphone, named the secondary path. This algorithm takes the name of filtered-X least mean squares (FXLMS) algorithm [12], and it will be illustrated in Section 2.1. The adaptive filter is introduced as a finite impulse response (FIR) filter, so in the z-transform domain, it is represented by a polynomial. However, in some cases, for example, when acoustic feedback from the control source to the reference microphone is present, it is necessary to model the poles of the physical system to avoid instability. On the other hand, the implementation of an infinite impulse response (IIR) filter, represented by a rational function in the z-transform domain, is able to model the poles of the system and overcome this problem, although the algorithm could converge to a solution that is not the absolute optimum. This kind of algorithm is called filtered-U recursive LMS (FURLMS) and is described in detail in Section 2.3.

In many applications, the disturbance source is not stationary and an increment of power can lead to the instability of the algorithm, if the step-size parameter is fixed to a large value. In this case, an FXLMS algorithm with step-size normalized with the power of the filtered reference signal (FXLMS with NSS) turns out to be useful, as will be described in Section 2.2.

When it is not possible to sense directly the signal of the source, the reference signal must be internally computed. The FXLMS algorithm applied to a feedback system of this kind is described in Section 2.4.

These algorithms will be applied to the multichannel ANC system schematized in Figure 1, composed of one reference microphone (for the feed-forward configurations only), two control loudspeakers, and two error microphones. This system works as described in the following:

- Two error microphones measure the error signals $e_1(n)$ and $e_2(n)$ and define the zone of quiet where the noise generated by the disturbance source has to be eliminated;
- For the case of feed-forward systems, the input microphone near the noise source measures a reference signal $x(n)$ before noise reaches the control loudspeakers; for feedback systems, this signal is internally modeled starting from $e_1(n)$ and $e_2(n)$;
- The control unit processes the measured data in real-time with the adaptive algorithm and calculates the output signals $y_1(n)$ and $y_2(n)$, which drive the two control loudspeakers;

- The control sources produce the computed signals that will be superimposed to the existing noise and will cancel it for interference.

In the following paragraphs this procedure, with the previously described algorithms, is illustrated in detail.
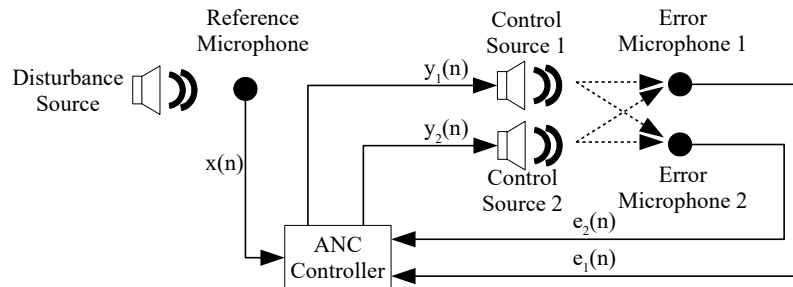

Figure 1. Schematic representation of the feed-forward system.

2.1. Filtered-X LMS Algorithm Applied to a Feed-Forward Configuration

Let us consider the physical system shown in Figure 2, composed of one reference signal $x(n)$, two error signals $e_i(n)$ ($i = 1, 2$), and two signals $y_j(n)$ ($j = 1, 2$) generated by the control sources. The impulse responses of the primary paths $p_i(n)$ describe the propagation of the reference signal from the source to the error microphones, where the noise disturbances $d_i(n)$ are detected. The signals produced by the control sources are transmitted through the secondary paths $s_{ji}(n)$ from the j-th source to the i-th microphone. They superimpose the existing noise disturbance $d_i(n)$, generating the error signals measured at the microphones. The figure also shows the impulse responses associated with the feedback paths $f_j(n)$ to indicate the physical possibility of reference signal corruption due to wave propagation from the control sources to the reference microphone. However, as depicted in Figure 2 and as required by the traditional FF_FXLMS algorithm, the output signals $v_j(n)$ are not computed nor processed by the control unit.
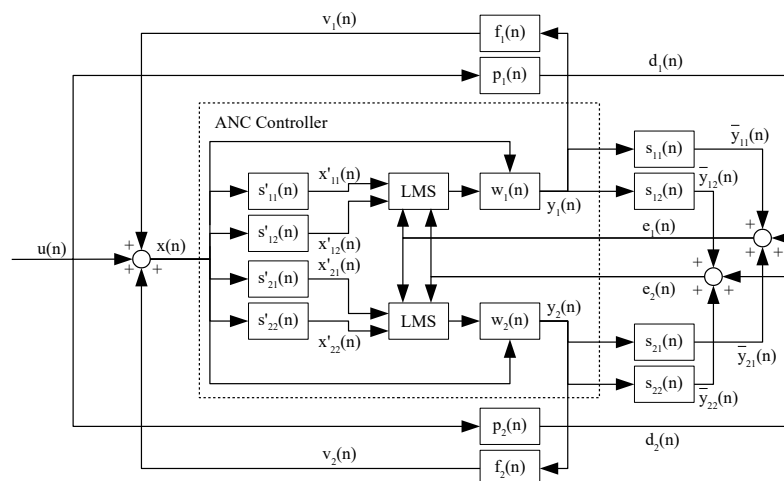

Figure 2. Schematic representation of FXLMS algorithm for a feed-forward configuration.

To correctly model the physical system and to guarantee stability, the FXLMS algorithm takes into account the presence of secondary paths inside the control unit. These impulse responses are estimated with the offline procedure reported in Section 2.1.1 and are saved as FIR filters $s'_{ji}(n) = [s'_{ji,0}(n)\ s'_{ji,1}(n)\ \dots\ s'_{ji,M-1}(n)]$, where M represents the length of secondary paths filters, assumed to be equal for all the filters. By means of these FIR filters, the (filtered) reference signals are computed as:

$$x'_{ji}(n) = \sum_{m=0}^{M-1} s'_{ji,m}(n)x(n-m). \tag{1}$$

The algorithm implemented in the ANC system minimizes the cost function $\xi(n)$, which represents the total amount of energy sensed by the error microphones:

$$\xi(n) = \sum_{i=1}^{2} e_i^2(n). \tag{2}$$

This can be achieved with an iterative procedure that modifies the adaptive filter coefficient vector $w_j(n) = [w_{j,0}(n)\ w_{j,1}(n)\ \ldots\ w_{j,K-1}(n)]$ of length K. In particular, the least mean squares approach translates the operation of cost function minimization in the updating expression of the adaptive coefficients shown in Equation (3):

$$w_{j,k}(n+1) = w_{j,k}(n) - \mu \sum_{i=1}^{2} e_i(n)x'_{ji}(n-k) \quad k = 0, 1, \ldots, K-1, \tag{3}$$

where μ is the step-size parameter, which regulates the convergence speed and determines the stability of the algorithm. Finally, the outputs of the algorithm that drive the two control sources are evaluated as:

$$y_j(n) = \sum_{k=0}^{K-1} w_{j,k}(n)x(n-k). \tag{4}$$

This procedure is repeated for any generic instant n.

2.1.1. Offline Estimation of Secondary Paths

Assuming the system to be linear time-invariant, it is possible to obtain an estimation $s'_{ji}(n)$ of the filters, characterizing the secondary paths, before the application of the active control. With reference to Figure 3, the procedure for the offline estimation is the following:

- A sample of white noise $y_j(n)$ is generated with the j-th control source and used as reference input for the adaptive filter $s'_{ji}(n)$ and for the coefficients updating in the LMS algorithm;
- The signal $e_i(n)$ is sensed with the i-th error microphone;
- The response of the adaptive model $e'_i(n)$ is computed as:

$$e'_i(n) = \sum_{m=0}^{M-1} s'_{ji,m}(n)y_j(n-m); \tag{5}$$

- The convergence error is evaluated as: $r_i(n) = e_i(n) - e'_i(n)$;
- The adaptive filter coefficients $s'_{ji}(n)$ are updated by using the LMS algorithm:

$$s'_{ji,m}(n+1) = s'_{ji,m}(n) + \mu r_i(n)y_j(n-m) \quad m = 0, 1, \ldots, M-1. \tag{6}$$

This procedure is repeated until a good convergence is reached. The coefficients of the adaptive filter $s'_{ji}(n)$ are saved and used for the active control procedure described in Section 2.1. Since the secondary paths are invariant during the ANC application, it is important to note that they do not consider modifications of the physical system, such as geometric, thermal, or boundary condition variations. To solve this problem, it is possible to apply an online estimation procedure [28] or a periodically used offline technique in order to update the secondary paths and take into account system variations. However, to limit the computational complexity, in this article, only the offline modeling of secondary paths is employed.
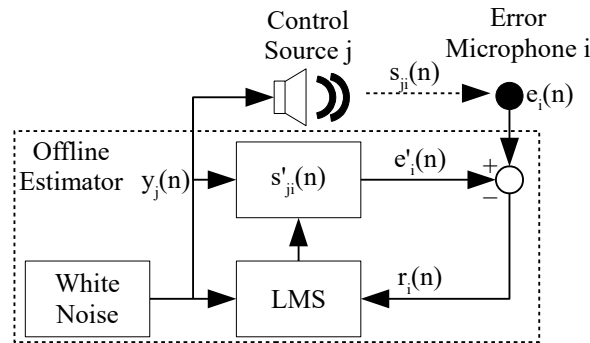
Figure 3. Schematic representation of the offline estimation procedure.

2.2. Filtered-X LMS Algorithm with Normalized Step-Size Applied to a Feed-Forward Configuration

In many applications, the power of the noise source is not stationary. Assuming a fixed step-size parameter in the FXLMS algorithm, the coefficients updating becomes slower as the power of the signal decreases, whilst instability can occur when the power increases. Many proposals can be found in the literature [18,22] to automate the process of choice of an adequate step-size parameter. For example, in [19], the step-size is normalized with respect to the power of the reference signal. However, this approach does not make it possible to take into account the effect of the secondary path filter applied to the reference signal. Other authors propose determining the step-size parameter as a function of the energy at the error microphone [20], even though in this case, the noise not coherent with the primary source could be included, altering the step-size evaluation. One of the best choices is computing a step-size parameter based on Griffiths' cross-correlation between the filtered reference signal and the error signal [21]. This approach makes it possible to vary the step-size parameter on the basis of the gradient of the updating coefficient, resulting in a robust algorithm, though the computational complexity for a multichannel system significantly increases. In this article, a normalization of the step-size with respect to the power of the filtered reference signal, as proposed in [29], is examined. In this case, Equation (3) must be substituted with Equation (7), in which the step-size parameters become functions of variable *n*:

$$w_{j,k}(n+1) = w_{j,k}(n) - \mu_j(n) \sum_{i=1}^{2} e_i(n) x'_{ji}(n-k) \quad k = 0, 1, \ldots, K-1. \tag{7}$$

The step-size parameters are evaluated at each time instant *n* as defined in Equation (8):

$$\mu_j(n+1) = \frac{\mu_{in}}{(M+K) \max_{i=1,2} \{P'_{ji}(n+1)\}}, \tag{8}$$

in which μ_{in} is an initial value and the power of the filtered reference signal P'_{ji} is updated with the following law:

$$P'_{ji}(n+1) = \beta P'_{ji}(n) + (1-\beta) \sum_{k=0}^{K-1} x'^2_{ji}(n-k), \tag{9}$$

where β is a "forgetting" factor ($0 \leq \beta < 1$), which determines the speed of updating of the step size. Low values of β are chosen when the reference signal is highly variable, while high values are preferred for stationary contests. The choice of the maximum power of the filtered reference signal $P'_{ji}(n)$ makes it possible to select the minimum step size, thus limiting the possibilities of instability, despite a slower convergence rate. For the application, the step-size parameters are constrained between two arbitrary limits: a maximum value μ_{max}, to avoid instability due to the large value of μ_j, and a minimum value μ_{min}, to avoid slow convergence and coefficients updating based on the quantization error associated with fixed-point math ($\mu_{min} \leq \mu_j(n) \leq \mu_{max}$).

2.3. Filtered-U Recursive LMS Algorithm Applied to a Feed-Forward Configuration

In some cases, the reference microphone could be exposed to the acoustic feedback generated by a control source. In such cases, it is necessary to take into account the feedback path of wave propagation from the control source to the reference microphone, because the formation of poles could make the system unstable. A simple extension of the FXLMS algorithm (FBFXLMS) was proposed [4], in which a sufficiently long FIR filter, usually estimated in a preliminary stage together with the secondary path, approximates the impulse response from the control source to the reference microphone. The contribution of the filtered control signal is afterward subtracted from what the microphone measures, reconstructing in this way the reference signal. Eriksson et al. proposed the use of an IIR filter [23] so that the poles of the adaptive filter remove the poles created by the acoustic feedback. This technique makes it possible to use a lower-order filter with respect to a FIR filter without a preliminary model of the feedback path that can be dynamically tracked during cancellation operations. However, these advantages come at the price of having filters that are not unconditionally stable and possible convergence to a local minimum of the cost function because the mean square error is generally non-quadratic.

Hereinafter, the application of an IIR filter with the recursive LMS (RLMS) algorithm is reported as developed by Feintuch [24]. Considering the scheme illustrated in Figure 4, after the preliminary stage of offline estimation of the secondary paths, the algorithm works as described in the following. The filtered reference signals are still computed as defined in Equation (1), while the filtered output signals are computed as:

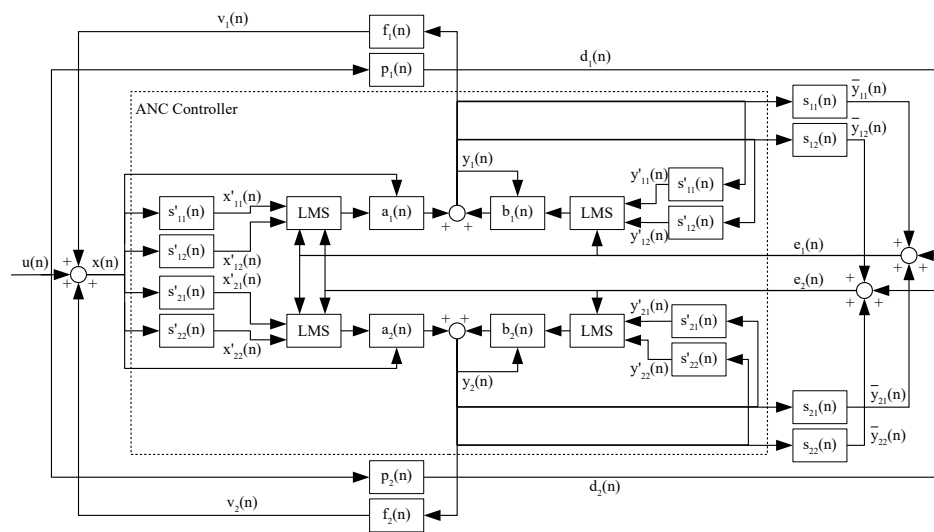$$y'_{ji}(n-1) = \sum_{m=0}^{M-1} s'_{ji,m}(n)y_j(n-m-1).\tag{10}$$

Figure 4. Schematic representation of FURLMS algorithm for a feed-forward configuration.

The updating law defined in Equation (3) is substituted by two updating equations, Equation (11) for the feed-forward coefficient vector $a_j(n) = [a_{j,0}(n)\ a_{j,1}(n)\ \dots\ a_{j,K-1}(n)]$ and Equation (12) for the feedback coefficient vector $b_j(n) = [b_{j,1}(n)\ b_{j,2}(n)\ \dots\ b_{j,K}(n)]$. Both vectors are assumed to have the same length K, whilst the two step-size parameters μ_a and μ_b are kept distinct for the two equations:

$$a_{j,k}(n+1) = a_{j,k}(n) - \mu_a \sum_{i=1}^{2} e_i(n)x'_{ji}(n-k) \quad k = 0, 1, \dots, K-1.\tag{11}$$

$$b_{j,k}(n+1) = b_{j,k}(n) - \mu_b \sum_{i=1}^{2} e_i(n)y'_{ji}(n-k) \quad k = 1, 2, \dots, K.\tag{12}$$

Finally, the two control signals are computed as in Equation (13):

$$y_j(n) = \sum_{k=0}^{K-1} a_{j,k}(n)x(n-k) + \sum_{k=1}^{K} b_{j,k}(n)y_j(n-k). \tag{13}$$

This procedure is repeated at any generic instant *n*.

2.4. Filtered-X LMS Algorithm Applied to a Feedback Configuration

The feedback system is typically implemented in all those situations in which the noise is predictable, for example, for the attenuation of transformer noise outdoors [25] or for the cancellation of fan noise [26]. Since the reference microphone is absent, the reference signal is internally modeled starting from the measurement of the error signal. The choice of this system makes it possible to contain the costs associated with the sensors and to protect the system against the acoustic feedback mentioned in the previous paragraphs. However, the feedback system generally provides a limited attenuation, in particular when the environment makes the modeling of the reference signal cumbersome, for example, in enclosed spaces. Moreover, this system is affected by amplification at high frequency due to an intrinsic phenomenon called waterbed effect [30], which could also lead to instability. Considering the scheme shown in Figure 5, the feedback system works as explained in the following. The filtered output signals are evaluated as:

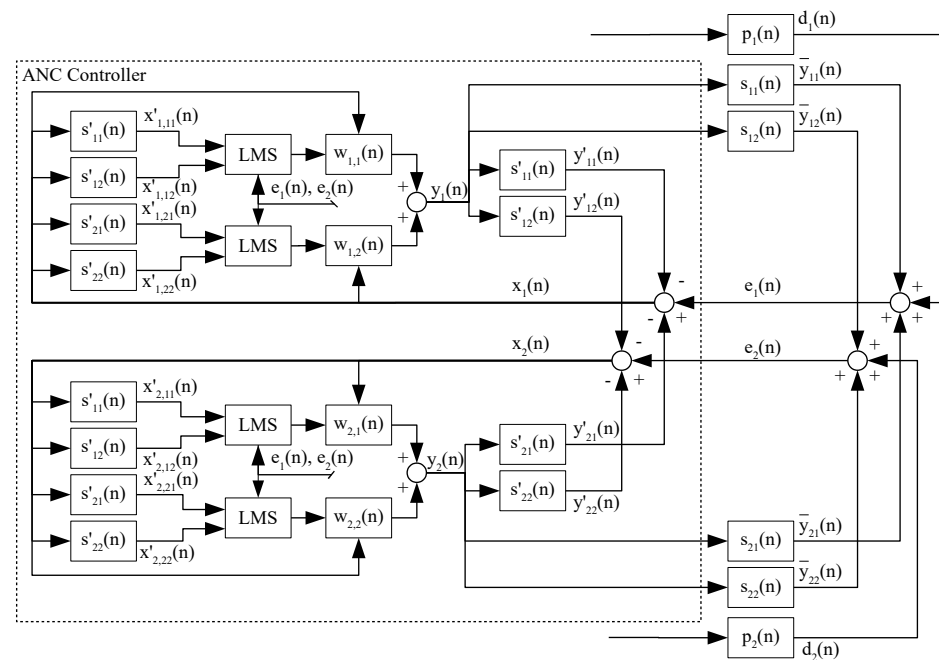$$y'_{ji}(n) = \sum_{m=0}^{M-1} s'_{ji,m}(n)y_j(n-m). \tag{14}$$

Figure 5. Schematic representation of FXLMS algorithm for a feedback configuration.

These contributions are subtracted from the error signals in order to model the reference signals, for which the subscript is changed from *i* to *l* for the sake of simplicity in the notation:

$$x_l(n) = x_i(n) = e_i(n) - \sum_{j=1}^{2} y'_{ji}(n). \tag{15}$$

The procedure becomes identical to the one of the feed-forward case described previously in Section 2.1. The filtered reference signals are thus computed as:

$$x'_{l,ji}(n) = \sum_{m=0}^{M-1} s'_{ji,m}(n)x_l(n-m). \tag{16}$$

The updating law presented in Equation (3) becomes:

$$w_{lj,k}(n+1) = w_{lj,k}(n) - \mu \sum_{i=1}^{2} e_i(n)x'_{l,ji}(n-k) \quad k = 0, 1, \ldots, K-1 \tag{17}$$

and, finally, the output signals are evaluated as:

$$y_j(n) = \sum_{l=1}^{2} \sum_{k=0}^{K-1} w_{lj,k}(n)x_l(n-k). \tag{18}$$

This procedure is repeated at any generic instant n.

3. Experimental Setup and Characterization

The experimental setup adopted for the tests, conducted in the hemi-anechoic chamber at the Engineering Department of the University of Ferrara, is reported in Figures 6 and 7. An omnidirectional noise source is placed outside the cabin, about 1 m away from it. The reference microphone, which measures the signal of the noise source in the feed-forward systems, has two possible locations: in front of the cabin, as shown in Figure 6a, or inside the cabin, as shown in Figure 7.
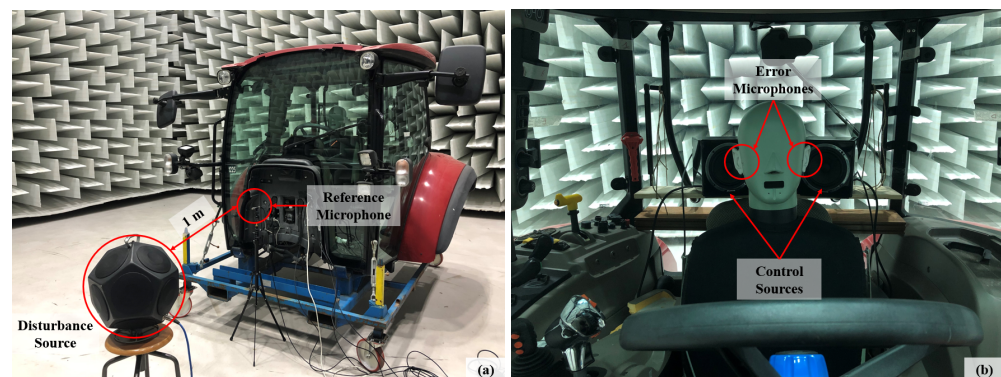
Figure 6. Experimental setup: (**a**) outside the cabin, (**b**) inside the cabin, with reference microphone placed outside.
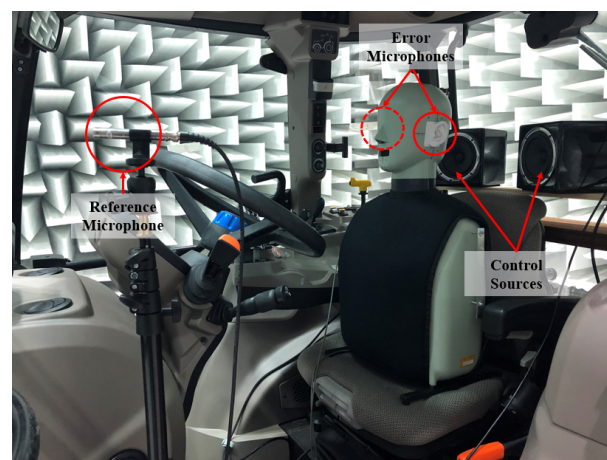

Figure 7. Experimental setup inside the cabin with the reference microphone placed inside.

For the feedback system, this microphone is not exploited, because the reference signals are modeled starting from the error signals. The error microphones, which define the zone of quiet, are allocated at the entrance to the ear canals of a binaural dummy torso

for acoustic testing, to take into account the diffraction effect due to the presence of the head. Two control loudspeakers with a cut-off frequency of 100 Hz, endowed with an amplifier and a 5.25″ driver, are positioned on a shelf mounted behind the seat, at the same height as the error microphones. The type of error microphones is 1/2″ B&K 4100, while for the reference, 1/2″ PCB 377B02 has been used. The whole system is driven by a National Instruments real-time target (cRio 9063) with an FPGA (field programmable gate array), sampling input and output signals with a frequency of 6400 Hz. The sensed data are processed in a deterministic way by means of the previously described algorithms, with a timing for the operations defined by the 40 MHz on-board clock. The tested algorithms are implemented on the hardware through LabVIEW, by compiling the codes directly on the FPGA to have a processing system working in an autonomous way with respect to the PC monitoring the experiments. During the compilation, the operations contained in the algorithms (i.e., the convolutions, sums, and subtractions as described in Section 2) are assigned to circuits able to work in parallel to optimize the processing time. All the arrays used for the storage of signals and filters are implemented on blocks of memory (BRAM), instead of look-up tables (LUT RAM), which would consume the more limited resources that the FPGA uses for the logical operations and employ a fixed-point data type to optimize the usage of resources with respect to floating-point data.

The generic scheme of the operations executed in the workflow is depicted in Figure 8. Firstly, all the arrays used for the storage of signals and filters are initialized to zero, while the length of the filters and the step size (for the algorithms with a fixed parameter) are updated from the external PC, which works as a simple interface. Secondly, the coefficients of the secondary paths are uploaded (considering the previously defined filter length), and the FPGA prepares itself to wait for "ANC On" command. At this point, the system works in a loop by processing the acquired data with the adaptive algorithm and generating the anti-noise signals in real time. When the "stop" command is sent to the FPGA, the loop is interrupted, and the stored data are transmitted to the external PC for the post-processing and the saving of the data.
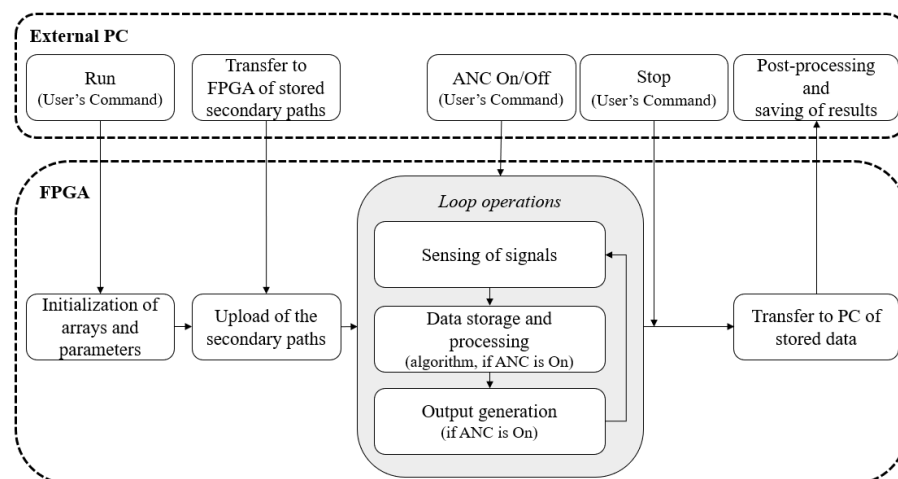
Figure 8. Generic scheme of the workflow implemented on the hardware.

The studied configurations with the respective algorithms are indicated in the following:

- Feed-forward configuration,
    - Filtered-X least mean squares (FF_FXLMS), as in Section 2.1;
    - Filtered-X least mean squares with normalized step size (FF_FXNLMS), as in Section 2.2;
    - Filtered-U recursive least mean squares (FF_FURLMS), as in Section 2.3;
- Feedback configuration,
    - Filtered-X least mean squares (FB_FXLMS), as in Section 2.4.

To compare these different algorithms, several signals are generated by the primary source:

- Pure tones at 100 Hz and 500 Hz;
- Pseudo-random noise, filtered up to 1000 Hz and with a period of 0.10 s;
- White noise filtered up to 1000 Hz.

4. Results and Discussion

In the following paragraphs, the results of the offline estimation of the secondary paths and the results of the ANC application for each of the considered signals are illustrated. All the tests have been carried out with filters of a length of 1024 elements both for secondary paths and adaptive coefficients. The step-size parameter is kept the same for all the algorithms that require a fixed value (FF_FXLMS, FB_FXLMS, FF_FURLMS), while it changes with respect to the signal type and the location of the reference microphone. The choice of the fixed step-size parameters represents the maximum value, which guarantees the convergence for all the algorithms. The step-size parameter values are reported in Table 1; it is worth pointing out that the choice of the rate does not represent the best choice in an absolute sense for each algorithm. Moreover, Table 2 shows the values of the parameters used in the FF_FXNLMS algorithm (μ_{max}, μ_{min}, μ_{in} and β) and the step size for the feedback coefficients updating (μ_b) in the FF_FURLMS algorithm, that are maintained the same in all the tests.

**Table 1.** Step-size parameters μ for algorithms with fixed value.

	100 Hz	500 Hz	Pseudo-Random	White Noise
External	0.120	0.700	0.500	0.500
Internal	1.000	5.000	5.000	5.000

Table 2. Parameters for the FF_FXNLMS and FF_FURLMS algorithms.

μ_b	μ_{max}	μ_{min}	μ_{in}	β
0.050	7.000	0.010	1.000	0.001

4.1. Results of the Secondary Paths Estimation

In Figure 9, the results of the offline estimation procedure are reported, considering a filter of length M = 1024 and a step size μ = 0.01. This evaluation was conducted once before the evaluation of the performance of the adaptive algorithms. Due to the low amplitude of the frequency response function of the control loudspeakers, the secondary paths show that, below 100 Hz, the system is not able to produce a sufficient amount of energy to attenuate the noise below this cut-off frequency. For this reason, the range where the active noise control system works is assumed to be between 100 Hz and a quarter of the sampling frequency (in this case 1600 Hz). In this range, the pressure nodes related to the modal response of the enclosure must be taken into account, because, at these frequencies, they could make the system ineffective due to local minima in the amplitude of the secondary paths. From the graphs, it is also possible to notice a similarity between the two direct paths (from control source *i* to error microphone *i*), shown on the left-hand side, and the crossed paths (from control source *i* to error microphone *j*), shown on the right-hand side, meaning a good symmetry of the problem.
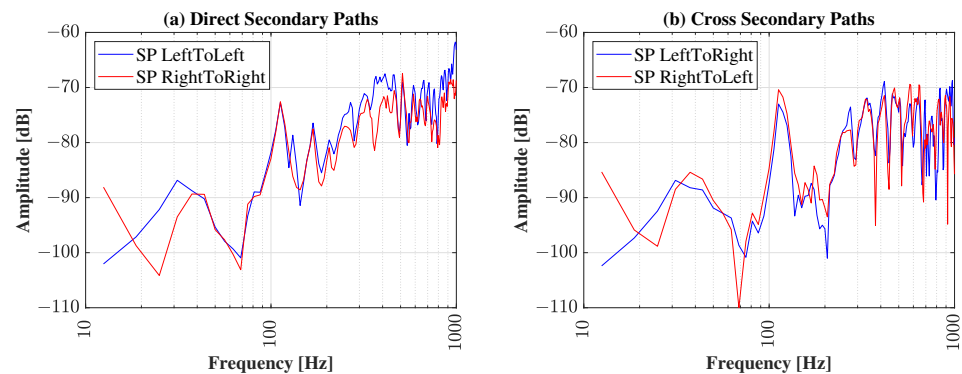
**Figure 9.** Amplitude of the frequency response function of the (**a**) direct and (**b**) cross secondary paths.

4.2. Results of the Active Control for Pure Tones

In this section, the results of the application of ANC to pure tones are described. It is well known that ANC for pure tones works very well, particularly for middle and low frequencies. However, this part is useful as an introduction to the practical problems in the studied configurations and as a reference for the successive more complex signals. Figure 10 illustrates a comparison between the ANC algorithms applied to a pure tone at 500 Hz. The results show that the feedback configuration is the slowest system to converge. Since the unique difference between the FB_FXLMS and FF_FXLMS algorithms consists of the way in which the reference signal is acquired, the slowness of the feedback system is attributed to its additional internal modeling of the reference signals. Moreover, some instability phenomena can be observed for the FB_FXLMS algorithm when the step-size parameter is increased, as shown on the right-hand side plot of Figure 10. The FF_FXLMS algorithm seems to exhibit a strong reduction in the speed of convergence when the reference microphone is moved inside the cabin. In reality, this behavior is not associated with the position of the reference microphone, but with the choice of the step size near the stability limit for the FF_FXLMS algorithm, making the convergence slower. On the other hand, FF_FURLMS is able to maintain a similar velocity thanks to its capability of considering the acoustic feedback coming from the control sources and corrupting the reference signal, while the FF_FXNLMS algorithm is able to preserve a similar performance thanks to the convergence to a smaller value of step size with respect to FF_FXLMS. As shown in Figure 11, the normalized step size varies in time when the active noise control is turned on, starting from a high value due to the transitory phase and converging in a few seconds to a stable value, which is calculated by adapting to the power of the reference signal, which is different between outside and inside.

The total attenuation within the first 15 s and the mean speed of convergence, expressed in dB/s and evaluated in the first second from the start of the active control, are summarized in Tables 3 and 4 for the conditions with external and internal reference microphone respectively. Considering the reference microphone outside the cabin, the FB_FXLMS exhibits the worst performance, both in terms of total attenuation and speed of convergence, for both the considered pure tones. When the reference microphone is inside the cabin, for a large wavelength (i.e., 100 Hz), the feed-forward algorithms, which do not consider possible acoustic feedback (i.e., FF_FXLMS and FF_FXNLMS), exhibit a decrease in their performance due to the influence of the sound generated by the control sources on the reference signal. On the other hand, as the frequency increases, the performance of the feed-forward algorithms increases, outperforming the FB_FXLMS approach. Finally, it should be pointed out that for disturbing tones with a small wavelength, the ANC becomes sensitive to the imperfections of the system, and a marked difference between the left ear and the right ear could be sensed.
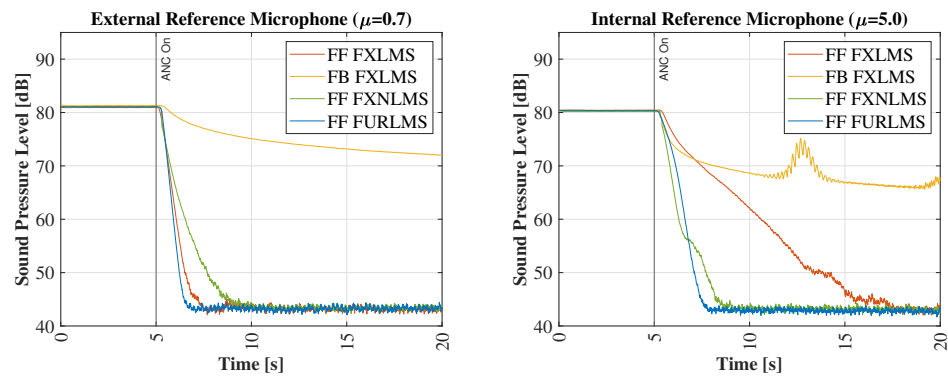
Figure 10. Time history of the left error signal amplitude for a pure tone at 500 Hz for external and internal reference microphone.
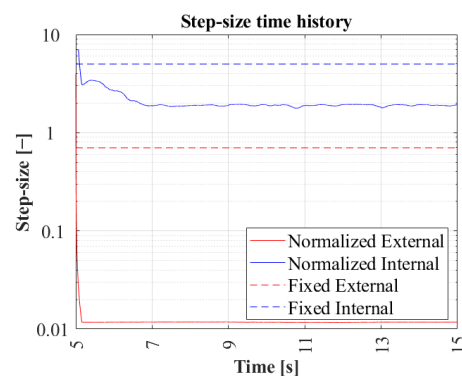
Figure 11. Example of time history of the step-size parameter for the FF_FXNLMS algorithm when active noise control is turned on and comparison with the fixed value.

Table 3. Attenuation and speed of convergence for external reference microphone for the pure tones.

| 100 Hz	FF_FXLMS		FB_FXLMS		FF_FURLMS		FF_FXNLMS	
Side	Left	Right	Left	Right	Left	Right	Left	Right
Reduction [dB]	45.0	45.4	7.0	6.1	42.5	42.3	44.0	32.6
Convergence [dB/s]	15.5	13.4	1.5	1.3	23.5	22.1	19.8	15.5
500 Hz	**FF_FXLMS**		**FB_FXLMS**		**FF_FURLMS**		**FF_FXNLMS**	
Side	Left	Right	Left	Right	Left	Right	Left	Right
Reduction [dB]	38.0	37.4	9.0	8.7	37.7	36.4	37.5	27.4
Convergence [dB/s]	23.8	23.0	2.4	2.8	29.4	28.0	14.1	8.4

Table 4. Attenuation and speed of convergence for internal reference microphone for the pure tones.

100 Hz	FF_FXLMS		FB_FXLMS		FF_FURLMS		FF_FXNLMS	
Side	Left	Right	Left	Right	Left	Right	Left	Right
Reduction [dB]	4.7	3.4	12.1	10.7	24.5	25.1	2.5	2.4
Convergence [dB/s]	2.4	1.8	5.0	4.3	9.2	6.3	1.4	1.5
500 Hz	**FF_FXLMS**		**FB_FXLMS**		**FF_FURLMS**		**FF_FXNLMS**	
Side	Left	Right	Left	Right	Left	Right	Left	Right
Reduction [dB]	37.2	37.8	14.0	12.8	37.6	37.4	37.1	34.9
Convergence [dB/s]	6.1	7.0	4.9	4.6	15.2	20.9	18.9	13.7

4.3. Results of the Active Control for Pseudo-Random Noise

The tests with pseudo-random signals are reported in Figure 12. This noise is composed of a broadband signal filtered up to 1000 Hz, repeated with a periodicity of 0.10 s. The period has been chosen in order to be lower than the duration modeled by the filters (computed as the number of elements of a filter divided by the sampling frequency) so that

the pseudo-random signal can be considered as an intermediate case study between the pure tone and the completely random noise. Furthermore, it should be pointed out that the results described in the following depend on the chosen bandwidth of the disturbing signal, since the convergence becomes slower with the increment of the bandwidth due to the higher complexity of the signals; moreover, by exceeding the limit of a quarter of the sampling frequency in the disturbance source, the instability of the system occurs. In this case, a low-pass filter directly applied to the reference signal to remove high frequencies would be beneficial to guarantee stability.
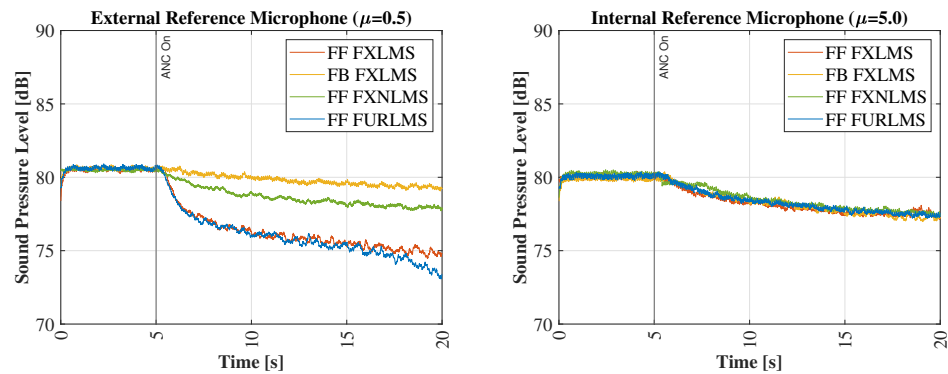
Figure 12. Time history of the left error signal amplitude for a pseudo-random noise signal filtered up to 1000 Hz and with period T = 0.10 s, for external and internal reference microphone.

For the case of the external reference microphone, the feed-forward systems with fixed step size (i.e., FF_FXLMS and FF_FURLMS) produce the best performance in terms of reduction and speed of convergence. Also in this case, the feedback system FB_FXLMS shows a slow convergence with the same step size of the feed-forward algorithms. When the reference microphone is inside the cabin, the performance exhibited by the different configurations becomes similar in terms of reduction and convergence velocity. The global results are presented in Tables 5 and 6. We can observe that the performance of all the feed-forward algorithms is reduced when the reference microphone is moved inside the cabin, while the feedback system FB_FXLMS increases its performance both in terms of total attenuation and speed of convergence, thanks to the increment of step size.

Table 5. Attenuation and speed of convergence for external reference microphone for the tested pseudo-random noise.

Pseudo-Random	FF_FXLMS		FB_FXLMS		FF_FURLMS		FF_FXNLMS	
Side	Left	Right	Left	Right	Left	Right	Left	Right
Reduction [dB]	5.4	4.5	1.2	1.0	6.4	5.6	2.6	1.9
Reduction [dB(A)]	13.9	9.5	1.0	0.5	14.2	9.8	7.2	3.5
Convergence [dB/s]	2.5	1.9	0.1	0.1	2.3	1.8	0.5	0.5

Table 6. Attenuation and speed of convergence for internal reference microphone for the tested pseudo-random noise.

Pseudo-Random	FF_FXLMS		FB_FXLMS		FF_FURLMS		FF_FXNLMS	
Side	Left	Right	Left	Right	Left	Right	Left	Right
Reduction [dB]	2.5	2.4	3.2	2.9	2.5	2.3	2.5	2.6
Reduction [dB(A)]	2.3	1.6	3.5	2.7	2.1	1.4	2.2	2.9
Convergence [dB/s]	0.7	0.6	0.8	0.7	0.6	0.6	0.1	0.1

4.4. Results of the Active Control for White Noise

Hereinafter, a completely random noise signal filtered up to 1000 Hz is used as a disturbance. However, all the successive conclusions are valid both for completely random

noise and pseudo-random noise signals, in which the period is greater than the duration modeled by the filters. For this kind of broadband noise, the achievement of a high level of reduction with an adaptive algorithm in a short time becomes difficult with respect to a periodic signal, as can be observed by comparing the results of the pseudo-random noise signal, given in Tables 5 and 6, with the results obtained for white noise and reported in Tables 7 and 8. In this latter case, the speed of convergence is not specified due to the high variability of the sound pressure level in time (fluctuations of ± 3 dB). The reduction in the performance for all the algorithms can be related to the LMS procedure: since the updating of the adaptive filters occurs in an iterative way, the lack of periodicity does not allow the coefficients to converge quickly to an optimal value, reducing the capability of attenuation. As illustrated in Figure 13, the feedback system FB_FXLMS is completely ineffective due to its predictor nature and shows some instability effects with amplification above 500 Hz, where the feed-forward systems generally show a higher efficiency and a better performance. The main contribution to the reduction of the overall A-weighted sound level is related to the band of 800 Hz (up to 10.1 dB of attenuation for FF_FXLMS and FF_FURLMS and 6.5 dB for FF_FXNLMS) for the case of external reference microphone, while for the internal position, it is associated with the band of 630 Hz (1.8, 1.2, and 2.1 dB, respectively for FF_FXLMS, FF_FURLMS, and FF_FXNLMS). As for the pseudo-random noise signal, it should be pointed out that the convergence speed depends on the bandwidth of the disturbing signal, which acts directly on the complexity of the signal. To improve these results, pre-calculated and non-adaptive filters should be employed, for instance, based on the optimization of the H_∞ norm [31–33].
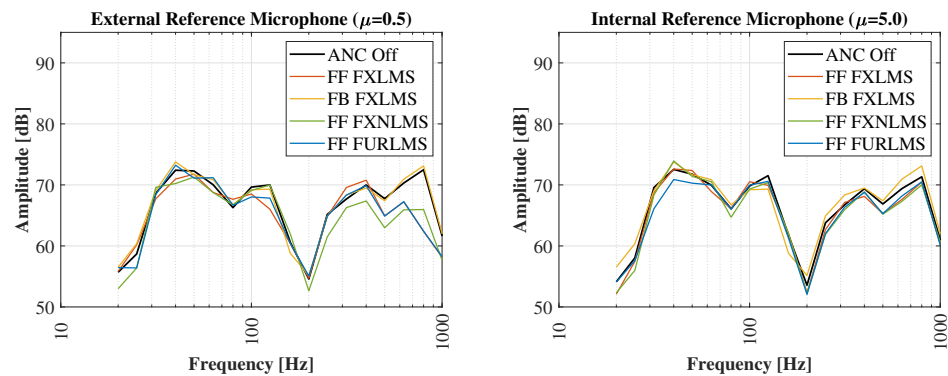

Figure 13. Spectral comparison for a white noise signal filtered up to 1000 Hz, for external and internal reference microphone.

Table 7. Attenuation for external reference microphone for the tested white noise.

White Noise	FF_FXLMS		FB_FXLMS		FF_FURLMS		FF_FXNLMS	
Side	Left	Right	Left	Right	Left	Right	Left	Right
Reduction [dB]	1.4	1.3	−0.3	−0.4	1.1	0.7	1.8	2.1
Reduction [dB(A)]	3.6	2.8	−0.4	−0.1	4.0	3.1	4.7	3.0

Table 8. Attenuation for internal reference microphone for the tested white noise.

White Noise	FF_FXLMS		FB_FXLMS		FF_FURLMS		FF_FXNLMS	
Side	Left	Right	Left	Right	Left	Right	Left	Right
Reduction [dB]	0.5	0.9	−0.5	−1.3	1.0	1.4	0.4	0.9
Reduction [dB(A)]	1.1	0.9	−1.4	−1.0	0.9	0.8	1.3	1.3

4.5. Comparison with a Free Field Case

The same type of experimental measurements have been carried out in a free field environment (i.e., in the hemi-anechoic chamber, without the cabin). For this scope, the power emitted by the disturbance source has been set in order to have a similar sound

pressure level at the position of the error microphones with respect to the case with the cabin, while the reference microphone has been brought nearer to the noise source, to guarantee a similar reference signal level. On the other hand, the distance between the disturbance source, the error microphones, and the control loudspeakers has been preserved; in this way, the attenuation provided by the ANC system is measured starting from a similar level of disturbance and can be compared for the cases with and without cabin. Since the reference microphone is directly exposed to the noise coming from the disturbance source, the step-size parameters of the "external" case have been used.

The results are reported in Table 9 for one pure tone (500 Hz), pseudo-random noise and white noise and should be compared with the results of Table 3, Table 5 and Table 7 respectively. Comparing the tables, it can be observed that all the algorithms are able to reach a higher level of attenuation in the free field case with respect to the case where the cabin is present, highlighting that the ANC system inside the small enclosure loses some of its performance due to the reflections of the walls.

Table 9. Attenuation and speed of convergence for a free field case for different types of noise.

500 Hz	FF_FXLMS		FB_FXLMS		FF_FURLMS		FF_FXNLMS	
Side	Left	Right	Left	Right	Left	Right	Left	Right
Reduction [dB]	46.4	45.4	16.0	12.9	49.1	46.7	45.8	43.6
Convergence [dB/s]	33.5	33.3	9.9	7.6	29.5	28.0	9.0	8.8
Pseudo-Random	FF_FXLMS		FB_FXLMS		FF_FURLMS		FF_FXNLMS	
Side	Left	Right	Left	Right	Left	Right	Left	Right
Reduction [dB]	7.5	7.2	5.1	6.4	9.5	7.4	4.0	3.3
Convergence [dB/s]	2.1	1.6	2.7	2.9	2.6	2.4	0.7	0.4
White Noise	FF_FXLMS		FB_FXLMS		FF_FURLMS		FF_FXNLMS	
Side	Left	Right	Left	Right	Left	Right	Left	Right
Reduction [dB]	2.2	2.0	1.4	1.9	2.4	2.1	1.3	1.2

For the case of pure tone, the algorithms FF_FXLMS, FB_FXLMS, and FF_FURLMS show a higher speed of convergence with respect to the case with the cabin, while FF_FXNLMS seems to be slower on the left side. However, this last consideration is valid only for the first second of convergence, where the speed is evaluated, since successively, the speed for the case with the cabin reduces faster than the free field case. Comparing the different algorithms, similar conclusions as in the case with the cabin can be drawn: FF_FXLMS, FF_FXNLMS, and FF_FURLMS have similar performance, while the FB_FXLMS algorithm exhibits the worst behavior both in terms of attenuation and speed of convergence due to its necessity of internally modeling the reference signal, making the algorithm slower.

For the analysis with the pseudo-random signal, the speed of convergence remains similar to the one evaluated in the case with the cabin for the FF_FXLMS, FF_FXNLMS, and FF_FURLMS algorithms. On the other hand, the speed increases for FB_FXLMS, becoming greater than that of the FF_FXNLMS algorithm.

Finally, for the white noise signal, the attenuation maintains the same order of magnitude for all the algorithms, smaller than the one calculated with the pseudo-random signal, with a little improvement for the FF_FXLMS, FB_FXLMS, and FF_FURLMS algorithms.

5. Conclusions

This article evaluates and compares the effectiveness of some of the most popular LMS-based algorithms applied to a multichannel ANC system, analyzing their performance in terms of speed of convergence and global attenuation of the disturbance for different kinds of signals. The experimental comparison has allowed us to evaluate some important practical aspects which would not otherwise be observable when using a computer simulation.

From the experimental comparison carried out on a small confined space (tractor cabin) in a hemi-anechoic chamber with a sound field generated by a dodecahedron placed outside the cabin, it is possible to observe that the best position for the reference microphone of the

feed-forward systems (i.e., FF_FXLMS, FF_FXNLMS, and FF_FURLMS) is outside the cabin since it provides a larger attenuation at a higher speed of convergence. This configuration also allows for greater stability, avoiding the acoustic feedback from the control loudspeakers to the reference microphone (present when the microphone is placed inside the cabin). Using the same step size for all the systems with a fixed parameter leads to slow convergence of the feedback system FB_FXLMS, due to the need for internal modeling of the reference signal. By incrementing the step size, the feedback system represents the solution most exposed to instability. For all the pure tones and the pseudo-random noise, the FF_FURLMS algorithm shows a higher convergence speed with respect to the other algorithms, since it implements IIR filters which consider the presence of poles in the filter modeling. The performance of all the configurations worsens when the external sound source emits a random signal with no periodicity rather than sinusoidal or pseudo-random signals. In particular, the feedback system becomes ineffective because of its predictor nature which is unsuitable for this kind of noise signal. On the other hand, the feed-forward systems can reach a reduction of more than 3 dB(A) on the overall level, acting on the frequency spectrum components above 500 Hz. Finally, the comparison with the same ANC system positioned in a free field shows that the presence of the cabin limits the capability of attenuation and in some cases the speed of convergence for all the LMS-based algorithms.

Author Contributions: Methodology, F.M., A.S. and P.B.; Investigation, F.M., A.S. and P.B.; Writing—original draft, F.M.; Writing—review & editing, A.S. and P.B.; Supervision, P.F. and F.P.; Project administration, P.F., F.P. and P.N. All authors have read and agreed to the published version of the manuscript.

Institutional Review Board Statement: Not applicable.

Informed Consent Statement: Not applicable.

Data Availability Statement: Some or all data and materials generated or used during this research are available from the corresponding author by reasonable request.

Conflicts of Interest: The authors declare no conflict of interest.

References

1. Jiang, J.; Li, Y. Review of active noise control techniques with emphasis on sound quality enhancement. *Appl. Acoust.* **2018**, *136*, 139–148. [CrossRef]
2. Kajikawa, Y.; Gan, W.S.; Kuo, S.M. Recent advances on active noise control: Open issues and innovative applications. *Apsipa Trans. Signal Inf. Process.* **2012**, *1*, e3. [CrossRef]
3. Qiu, X.; Lu, J.; Pan, J. A new era for applications of active noise control. In Proceedings of the Internoise 2014—The 43rd International Congress on Noise Control Engineering, Melbourne, Australia, 16–19 November 2014; pp. 1–10.
4. Kuo, S.M.; Panahi, I.; Chung, K.M.; Horner, T.; Nadaski, M.; Chyan, J. Design of active noise control systems with the TMS320 family. *Tex. Instruments*. 1996. Available online: https://www.researchgate.net/publication/228705078_Active_noise_control_systems_with_the_TMS320_family (accessed on 6 June 2023).
5. Oh, S.H.; Park, Y.; Rhee, S.W.; Kim, S.H. Design criteria of feedback controller for hybrid control with parametric uncertainty. In Proceedings of the Internoise 2003—The 32nd International Congress and Exposition on Noise Control Engineering, Seogwipo, Republic of Korea, 25–28 August 2003; pp. 482–489.
6. Lopez-Caudana, E.; Betancourt, P.; Cruz, E.; Nakano-Miyatake, M.; Perez-Meana, H. An active noise cancelling algorithm with secondary path modeling. In Proceedings of the 12th WSEAS International Conference on Computers, Heraklion, Greece, 23–25 July 2008; pp. 194–199. [CrossRef]
7. Sano, H.; Inoue, T.; Takahashi, A.; Terai, K.; Nakamura, Y. Active control system for low-frequency road noise combined with an audio system. *Proc. IEEE Trans. Speech Audio Process.* **2001**, *9*, 755–763. [CrossRef] [PubMed]
8. Li, Z.; Li, C.; Wei, X.; Cheng, J.; Wang, Y.; Yu, Y.; Lai, Y.; Hu, Z. Active noise control in the application of large suction side type range hood. In Proceedings of the Inter-Noise 2017—46th International Congress and Exposition on Noise Control Engineering, Hong Kong, China, 27–30 August 2017; Volume 2017, pp. 2757–2762.

9. Samarasinghe, P.N.; Zhang, W.; Abhayapala, T.D. Recent advances in active noise control inside automobile cabins: toward quieter cars. *IEEE Signal Process. Mag.* **2016**, *33*, 61–73. [CrossRef]

10. Hasegawa, S.; Tabata, T.; Kinoshita, A.; Hyodo, H. The development of an active noise control system for automobiles. In Proceedings of the Worldwide Passenger Car Conference and Exposition, Dearborn, MI, USA, 28 September–1 October 1992. [CrossRef]

11. Lee, S.K.; Lee, S.; Back, J.; Shin, T. A new method for active cancellation of engine order noise in a passenger car. *Appl. Sci.* **2018**, *8*, 1394 . [CrossRef]

12. Mori, F.; Fausti, P.; Pompoli, F.; Santoni, A.; Bonfiglio, P. Experimental tests of a multichannel active noise control system for the cancellation of engine noise applied to the cabin of a tractor. In Proceedings of the 28th International Congress on Sound and Vibration, Singapore, 24–28 July 2022.

13. Fanigliulo, R.; Del Duca, L.; Fornaciari, L.; Grilli, R.; Tomasone, R.; Pochi, D. Efficiency of an ANC system in the tractor cabin under controlled engine workload. *Noise Control. Eng. J.* **2020**, *68*, 339–357. [CrossRef]

14. Gulyas, K.; Pinte, G.; Augusztinovicz, F.; Desmet, W.; Sas, P. Active noise control in agricultural machines. In Proceedings of the ISMA 2002, Leuven, Belgium, 16–18 September 2002.

15. Carme, C.; Fohr, F.; Besombes, M. Active noise reduction in the cabin of an earth-moving machine. In Proceedings of the 2002 Internetional Congress and Exposition on Noise Control Engineeing, Dearborn, MI, USA, 19–21 August 2002.

16. Zhu, L.; Yang, T.; Li, X.; Pang, L.; Zhu, M. Active control of broadband noise inside a car using a causal optimal controller. *Appl. Sci.* **2019**, *9*, 1531 . [CrossRef]

17. Bambang, R.; Uchida, K.; Bayu, W. Active noise control in three dimension space using diagonal recurrent neural networks. In Proceedings of the Inter-Noise 2003—The 32nd International Congress and Exposition on Noise Control Engineering, Seogwipo, Republic of Korea, 25–28 August 2003.

18. Bismor, D.; Czyz, K.; Ogonowski, Z. Review and comparison of variable step-size LMS algorithms. *Int. J. Acoust. Vib.* **2016**, *21*, 24–39. [CrossRef]

19. Veeravasantarao, D.; Ajay, S.; Kumar, P.P.; Behera, L. Adaptive active noise control schemes for headset applications. *Proc. Ifac Proc. Vol.* **2008**, *41*, 7550–7555. [CrossRef]

20. Kwong, R.H.; Johnson, E.W. A variable step size LMS adaptive algorithm. *Proc. IEEE Trans. Signal Process.* **1992**, *40*, 1633–1642. [CrossRef]

21. Narasimhan, S.V.; Veena, S.; Lokesha, H. Variable step-size Griffiths' algorithm for improved performance of feedforward/feedback active noise control. *Signal Image Video Process.* **2010**, *4*, 309–317. [CrossRef]

22. Bharath, Y.K.; Chitralekha, G.; Veena, S.; Lokesha, H.; Nagalakshmi, K.V.; Dilna, U. Robust active noise control system for fighter aircraft pilot helmet application. *Proc. Procedia Comput. Sci.* **2016**, *89*, 690–699. [CrossRef]

23. Eriksson, L.J.; Allie, M.C.; Greiner, R.A. The selection and application of an IIR adaptive filter for use in active sound attenuation. *Proc. IEEE Trans. Acoust. Speech Signal Process.* **1987**, *35*, 433–437. [CrossRef]

24. Feintuch, P.L. An adaptive recursive LMS filter. *Proc. Proc. IEEE* **1976**, *64*, 1622–1624. [CrossRef]

25. Tao, J.; Qiu, X.; Pan, J. Control of transformer noise using an independent planar virtual sound barrier. In Proceedings of the Acoustics 2015 Hunter Valley, Hunter Valley, Australia, 15–18 November 2015 ; pp. 1–10.

26. Liu, X.W.; Chang, C.Y.; Kuo, S.M. Development of active noise control systems for centrifugal fans. In Proceedings of the Inter-Noise 2017—46th International Congress and Exposition on Noise Control Engineering, Hong Kong, China, 27–30 August 2017; pp. 2763–2769.

27. Kuo, S.M.; Morgan, D.R. Active noise control: A tutorial review. *Proc. IEEE* **1999**, *87*, 943–973. [CrossRef]

28. Yi, S.Z.; Fei, R.Y.; Zhou, D.S.; Liu, T.W.; Yu, J.P.; Yang, J.F.; Gong, K.C. New method to improve the secondary path modeling accuracy for active noise control systems. In Proceedings of the Internoise 2003—The 32nd International Congress and Exposition on Noise Control Engineering, Seogwipo, Republic of Korea, 25–28 August 2003; pp. 474–481.

29. Sharma, M.K.; Vig, R.; Pal, R.; Shantharam, V. Quiet zone for the patient in an ambulance: Active noise control technology for siren noise reduction. *Arch. Acoust.* **2018**, *43*, 275–281. [CrossRef]

30. Paurobally, R.; Pan, J. Practical active noise control - Results and difficulties. In Proceedings of the 12th International Congress on Sound and Vibration 2005, Lisbon, Portugal, 11–14 July 2005; Volume 1, pp. 506–513.

31. Mehta, P.; Zheng, Y.; Hollot, C.; Chait, Y. Active noise control in ducts: Feedforward feedback design by blending H_∞ and QFT methods. In Proceedings of the The 13th Triennial World Congress IFAC, San Francisco, CA, USA, 30 June–5 July 1996.

32. Loiseau, P.; Chevrel, P.; Yagoubi, M.; Duffal, J. Broadband active noise control design through nonsmooth H_∞ synthesis. *Proc. IFAC Pap. Online* **2015**, *48*, 396–401. [CrossRef]

33. Boultifat, C.; Loiseau, P.; Chevrel, P.; Lohéac, J.; Yagoubi, M. FXLMS versus H_∞ control for broadband acoustic noise attenuation in a cavity. *Proc. IFAC Pap. Online* **2017**, *50*, 9204–9210. [CrossRef]